J Nanopart Res (2009) 11:41–53
DOI 10.1007/s11051-008-9452-6

Neurotoxicity of low-dose repeatedly intranasal instillation of nano- and submicron-sized ferric oxide particles in mice

Bing Wang · Weiyue Feng · Motao Zhu · Yun Wang · Meng Wang · Yiqun Gu · Hong Ouyang · Huajian Wang · Ming Li · Yuliang Zhao · Zhifang Chai · Haifang Wang

Received: 2 June 2008 / Accepted: 6 June 2008 / Published online: 25 June 2008

Abstract Olfactory tract has been demonstrated to be an important portal for inhaled solid nanoparticle transportation into the central nervous system (CNS). We have previously demonstrated that intranasally instilled Fe_2O_3 nanoparticles could transport into the CNS via olfactory pathway. In this study, we investigated the neurotoxicity and size effect of repeatedly low-dose (130 μg) intranasal exposure of nano- and submicron-sized Fe_2O_3 particles (21 nm and 280 nm) to mice. The biomarkers of oxidative stress, activity of nitric oxide synthases and release of monoamine neurotransmitter in the brain were studied. Our results showed that significant oxidative stress was induced by the two sizes of Fe_2O_3 particles. The activities of GSH-Px, Cu,Zn-SOD, and cNOS significantly elevated and the total GSH and GSH/GSSG ratio significantly decreased in the olfactory bulb and hippocampus after the nano- and submicron-sized Fe_2O_3 particle treatment ($p < 0.05$). The nano-sized Fe_2O_3 generally induced greater alteration and more significant dose–effect response than the submicron-sized particle did. Some slight perturbation of monoamine neurotransmitters were found in the hippocampus after exposure to the two sizes of Fe_2O_3 particle. The TEM image showed that some ultrastructural alterations in nerve cells, including neurodendron degeneration, membranous structure disruption and lysosome increase in the olfactory bulb, slight dilation in the rough endoplasmic reticulum and lysosome increase in the hippocampus were induced by the nano-sized Fe_2O_3 treatment. In contrast, in the submicron-sized Fe_2O_3 treated mice, slightly swollen mitochondria and some vacuoles were observed in the olfactory bulb and hippocampus, respectively. These results indicate that intranasal exposure of Fe_2O_3 nanoparticles could induce more severe oxidative stress and nerve cell damage in the brain than the larger particle did. This is the first study to compare the neurotoxicity of nano- and submicron-sized Fe_2O_3 particles in the central nervous system after long-term and low-dose intranasal exposure.

B. Wang · W. Feng (✉) · M. Zhu · Y. Wang · M. Wang · H. Ouyang · H. Wang · M. Li · Y. Zhao (✉) · Z. Chai
Laboratory for Bio-Environmental Effects of Nanomaterials and Nanosafety and Key Laboratory of Nuclear Analytical Techniques, Institute of High Energy Physics, Chinese Academy of Sciences, Beijing 100049, China
e-mail: fengwy@mail.ihep.ac.cn

Y. Zhao
e-mail: zhaoyuliang@mail.ihep.ac.cn

M. Zhu · Y. Wang · M. Wang · H. Wang · M. Li
Graduate School of Chinese Academy of Sciences, Beijing 100049, China

Y. Gu
Maternity Hospital of Haidian District, Beijing 100080, China

H. Wang
College of Chemistry and Molecular Engineering, Peking University, Beijing 100871, China

Keywords Neurotoxicity · Ferric oxide nanoparticle · Submicron-sized · Central nervous system · Mice · Nanotechnology · Occupational health · EHS

Introduction

In recent years, considerable attention has been paid to investigate the health impact of occupational and environmental "ultrafine" particles (UFP), particles with size less than 100 nm in aerodynamic diameter, due to the rapid development of nanotechnology (Maynard and Kuempel 2005). Through many detailed investigations in human beings and animals, it has been made great progress in understanding the associations of UFPs with respiratory and cardiovascular diseases (Donaldson et al. 2001; Donaldson and Stone 2003; MacNee and Donaldson 2003). It is known that spherical solid particles can be inhaled when their aerodynamic diameter is less than 10 μm. The smaller the particulates are, the deeper the particulates travel into the respiratory tract and the lower the clearance rate of these particles remove from the deposition sites (Hoet et al. 2004). Although respiratory system is considered to be the main portal of entry for inhaled ultrafine particles (Peters et al. 1997; Utell and Frampton 2000), extrapulmonary translocation after respiratory tract deposition is likely to happen via accidental or occupational acute exposure (Nemmar et al. 2001). It is also possible that inhaled UFPs, by virtue of their extremely small size may deposit in the olfactory mucosa and then translocate in the central nervous system (CNS), which in turn might cause neurotoxicity. Recent studies support the concept that the CNS may be an important target organ for nanoparticle extrapulmonary translocation after respiratory exposure (Oberdörster et al. 2004; Elder et al. 2006). However, the studies about the effects of nanoparticles on CNS are still limited (Elder et al. 2006; Tin-Tin-Win-Shwe et al. 2006; Oberdörster 2004).

It has been proposed that the transitional metal in the particulate matter might play an important role in the CNS diseases (Bush 2003). Some evidences indicate that iron accumulation in brain is an initial event causing neuronal death or is a consequence of some neurodegenerative disease processes including Hallervorden-Spatz, Parkinson's disease (PD) and Alzheimer's disease (AD) (Aisen et al. 1999; Thompson et al. 2001; Qian and Shen 2001). Iron nanomaterials with super-paramagnetic characteristics and high catalytic abilities have been suggested many potential applications in industry, environment, and biomedicine such as photocatalysis, bioremediation and biomedical imaging and so forth (Horányi and Kálmán 2004; Penpolcharoen et al. 2001). However, a recent investigation indicated that exposure to anionic magnetic nanoparticles resulted in a dose-dependent reduction ability of pheochromocytoma cell line (PC12) differentiation in response to the nerve growth factor (Pisanic et al. 2007).

In our previous study, we demonstrated that intranasally instilled Fe_2O_3 nanoparticle could transport into the brain via olfactory route (Wang et al. 2007). In this work, we investigated the size-related neurotoxicity in mice after repeatedly intranasal exposure to low-dose of nano- and submicron-sized Fe_2O_3 particles. The particle-induced oxidative stress in sub-brain regions was evaluated by several oxidative stress biomarkers. The alterations in brain monoamine neurotransmitter release were measured. The changes in ultrastructure of nerve cells in brain regions were observed by transmission electron microscopy (TEM).

Materials and methods

Characterization of nano- and submicron-sized ferric oxide particle

Two engineered ferric oxide particles (21 nm and 280 nm) were purchased from Nanjing Haitai Nanomaterial Co. Ltd, and Chengdu Shi-Jia-Wei-Er Co. Ltd, China, respectively. The size and shape of the particles were characterized by transmission electron microscopy (TEM, JEOL JEM-200CX). The purity of the particles was analyzed by ICP-AES technique (Baird ICP2070, USA). The crystal structure of the particles was measured by the Philips X'Pert PRO Multipurpose X-ray powder diffractiometer with Co $K\alpha$ ($\lambda = 0.179$ nm) radiation and a solid state X'Celerator. The scanning rate was 0.05°/min.

The nano- and submicron-sized Fe_2O_3 particles were dispersed in physiological saline solution containing 0.1% sodium carboxy methyl cellulose (SCMC) and ultrasonic vibrated for 5–7 min. In

order to obtain a homogenized suspension, the dispersion solution was stirred on vortex agitator before every use. The hydrodynamic diameters of the particles in the dispersion solution were measured by a 90Plus Particle Size Analyzer (PSA) (Brookhaven Instrument Corp, USA).

Animal and experimental design

The healthy CD-ICR male mice of 4-week-old and 20–22 g body weight were supplied by the Department of Laboratory Animal Science, Peking University Health Center. The mice were fed sterilized commercial pellet diet and deionized water ad libitum, and kept in plastic cages in a 20 ± 2 °C and 50–70% relative humidity room with a 12-h light/dark cycle. The animal experiments were carried out in accordance with the Guiding Principles in the Use of Animals in Toxicology adopted by Society of Toxicology.

Based on the permissible exposure limit (PEL) for iron oxide fume (10 mg/m^3 for 8 h/day exposure) set by Occupational Safety and Health Administration, the total permissible dose of Fe_2O_3 fume for a 20-g-weight mouse is calculated as 1.31 mg/day. In our study, a total amount of 130 μg of 21 nm- or 280 nm-Fe_2O_3 particles, ten times lower than the permissible inhalable dose for mouse, were intranasally instilled into two nostrils of the mice every other day. After 12 h, 72 h, 14 days, and 30 days instillation, the brain of mice was collected and further divided into olfactory bulb, hippocampus, cortex, cerebellum, and brain stem. The sub-brain samples were quickly frozen in liquid nitrogen and then stored at −70 °C until use. The GSH-Px, total GSH, GSSG, and GSH/GSSG ratio were assayed at 12 h, 72 h, and 14 days of instillation. Considering the low levels of SOD, NOS, TBARS and monoamine neurotransmitters in brain, their activities and contents were analyzed in the 30-day exposed samples. Two samples of olfactory bulb and hippocampus of 30 days instillation were kept in 2% glutaraldehyde (4 °C) for TEM study.

Sub-brain homogenate preparation

The olfactory bulb, hippocampus, cortex, cerebellum, and brain stem were homogenized in a 50-mmol/L cold Tris–HCl buffer (pH = 7.47) containing 1 mmol/L EDTA and 0.25 mmol/L sucrose and sonicated with an Ultrasonic Cell Disrupter (Ningbo Scientz Biotechnology Co. Ltd). The homogenates were centrifuged at 10,000*g* for 10 min at 4 °C and the supernatant was collected for oxidative stress biochemical assay. Protein contents in the supernatant were determined by the method of Bradford (Bradford 1976).

Oxidative-stress-related biomarker assay

GSH-Px

GSH-Px activity was measured by quantifying the rate of H_2O_2-induced oxidation of GSH to oxidized glutathione (GSSG) under the existence of GSH-Px based on the modified method of 5,5-dithiobis-2-nitrobenzoic acid (DTNB) (Flohe and Gunzler 1984).

GSH and GSSG

Total glutathione (GSH) and oxidative glutathione (GSSG) levels were measured by the colorimetric microplate assay kits supplied by Beyotime Institute of Biotechnology, Zhejiang, China. Briefly, 40 μL metaphosphoric acid was added into 10 μL sub-brain homogenates and then centrifuged at 10,000*g* for 10 min at 4 °C. The supernatant was used for GSH and GSSG assay. The total GSH level was measured by the method of DTNB-GSSG recycling assay (Baker et al. 1990). The GSSG level was quantified by the same method of total GSH assay after the supernatant was pretreated with 1% 1 mol/L 2-vinylpyridine solution to remove the reduced GSH. The amount of reduced GSH was obtained by subtracting the amount of GSSG from that of the total GSH.

SOD

The activity of superoxide dismutase (SOD) was measured at 550 nm as the rate of inhibiting the reduction of nitrotetrazolium blue when superoxide anion radical was generated during the oxidation of xanthine by xanthine oxidase (Sun et al. 1988). The Cu,Zn-SOD activity was measured when the sample was treated with 2% SDS to inhibit the Mn-SOD activity (Misra and Fridovich 1972). The difference values between the total SOD and Cu,Zn-SOD activity was considered as Mn-SOD activity.

NOS

The activities of total nitric oxide synthase (T-NOS) in sub-brain homogenates were spectrophotometrically measured with a commercial-available kit (Nanjing Jiancheng Bioengineering Institute, Jiangsu, China) based on the oxidation of oxyhaemoglobin to methaemoglobin by nitric oxide (Salter et al. 1991). The inducible NOS (iNOS, calcium-independent) activity was measured by adding ethylene glycol-bis-(2-aminoethyl)-*N*,*N*,*N*′, *N*′-tetraacetic acid (EGTA) to chelate free Ca^{2+} in the reaction mixture. The constitutive NOS (cNOS, calcium-dependent) activity was calculated by subtracting iNOS from T-NOS. The NOS activities were expressed as units per miligram protein.

TBARS

The contents of lipid peroxides product in brain samples were determined by the method of thiobarbituric acid reactive substances (TBARS) (Ohkawa et al. 1979). The concentration of TBARS was calculated by a calibration curve using 1,1,3,3′-tetraethoxy propane as a standard and expressed as nanomole per gram tissue.

All spectrophotometric measurements were carried out in a multifunctional-microplate-based spectrophotometric reader (Spectramax M2 spectrophotometer, Molecular Devices Corporation, America).

Monoamine neurotransmitter and their metabolites determination

Six mice per group were killed at the 30th day of instillation, the hippocampus was removed and immediately sonicated in cold 0.1 mol/L $HClO_4$ containing 134 μmol/L EDTA and 263 μmol/L $Na_2S_2O_5$ for 30 s. The homogenate was centrifuged at 12,000*g* for 20 min at 4 °C. The 20 μL supernatant was applied to an HPLC-ECD (Shimadzu, Kyoto, Japan) to determine the concentrations of monoamine neurotransmitter and their metabolites, including dopamine (DA) and its metabolite 3,4-dihydroxyphenylacetic acid (DOPAC), homovanillic acid (HVA), 5-hydroxytryptamine (5-HT) and its metabolite 5-hydroxyindoleacetic acid (5-HIAA), and norepinephrine (NE). The 0.1 mol/L sodium acetate/0.01 mol/L citric acid buffer (pH 4.8) containing 0.25 mol/L disodiummedetate, 0.4 mol/L dibutylamine, 1 mol/L sodium octyl sulfate and 82% methanol (v/v) was used as elution solution. The flow rate was 0.8 mL/min.

Transmission electron microscopy (TEM) study

A small block ($\sim$1 mm^3) of sub-brain samples were fixed in 2% glutaraldehyde (pH 7.3) overnight, then the samples were treated according to the general protocols for TEM study (Au et al. 2002). The ultra-thin sections (70–100 nm) were stained with lead citrate and uranyl acetate and were observed by JEOL JEM-100CX II electron microscopy.

Statistical analysis

All data were expressed as means ± standard deviation. The test of one-way variance (ANOVA) followed by LSD or Tamhane's T2 test in SPSS package program (Version 11.0) was used to detect the significant difference between the treated groups and the control. The *p*-values less than 0.05 were considered statistically significant.

Results

Particle characterization

The results of TEM indicated that the primary sizes of the nano- and submicron-sized Fe_2O_3 particles were about 21 ± 6 nm and 280 ± 80 nm, respectively, similar to the data of size provided by the manufacturers (Fig. 1). The shapes of the two-sized Fe_2O_3 particles were near spherical (Fig. 1). The purity determined by ICP-AES showed that only trace amount of some transition metals, such as Co, Cr, Cu, Mn and Zn could be detected in the particles. The purities of the two-sized Fe_2O_3 particles were higher than 99%. The X-ray powder diffraction (XRD) analysis indicated that the nano- and submicron-sized Fe_2O_3 particles exhibited the crystal structural of α-Fe_2O_3 (Fig. 2). The particle size distribution measured by DLS showed that the 21 nm-Fe_2O_3 particles in 0.1% SCMC physiological saline solution were nearly monodisperse with the mean diameter of 21 ± 4 nm (Fig. 3) that was consistent with the results by TEM. Versus the 21 nm-Fe_2O_3, the 280 nm-Fe_2O_3 particles in the

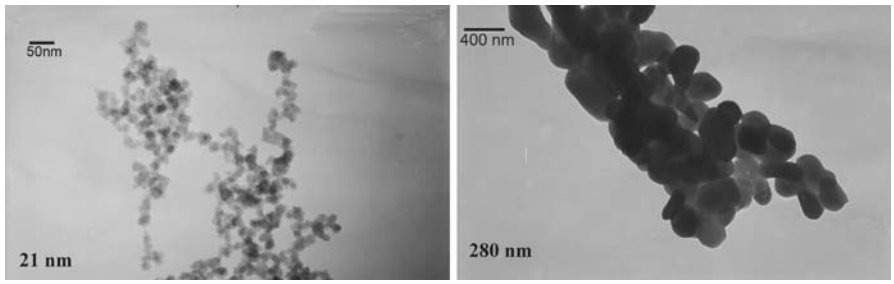

Fig. 1 TEM images of 21 nm- and 280 nm-Fe_2O_3 particles

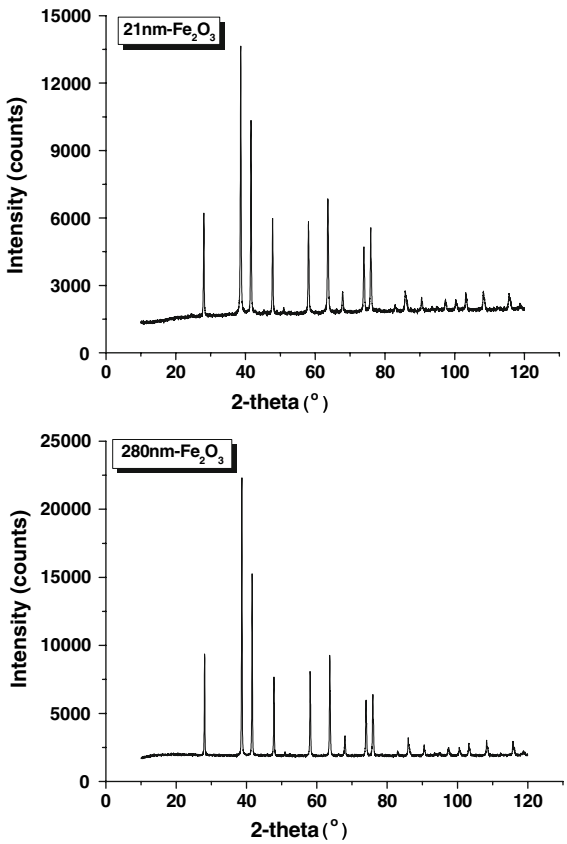

Fig. 2 X-ray powder diffraction study of iron oxide particles. 21 nm- and 280 nm-Fe_2O_3 particles exhibited the crystal structural of α-Fe_2O_3

dispersion medium showed a wider size distribution (Fig. 3) that about 10% of the particles were in the range of 44–102 nm in the dispersing solution, and about 90% were in 113–291 nm.

Oxidative stress in CNS

After low-dose repeatedly intranasal exposure of the nano- and submicron-sized Fe_2O_3 particles, the GSH-Px activities were significantly increased by 1.5-fold in the olfactory bulb and 2-fold in the hippocampus of 21 nm-Fe_2O_3 instilled mice at 12 h post-instillation when compared with the control ($p < 0.05$) (Fig. 4). Comparatively, 50% and 80% significant increase of GSH-Px activities were observed in the olfactory bulb and hippocampus in the 280 nm-Fe_2O_3 instilled mice at 12 h post-instillation ($p < 0.05$), respectively. Besides the olfactory bulb and hippocampus, 21 nm-Fe_2O_3 induced a slight increase of GSH-Px activities in the cortex as well, but no statistical difference was found versus the control.

The 21 nm-Fe_2O_3 instilled mice were found to have 44% and 49% decline of GSH in the olfactory bulb and hippocampus, respectively, comparing with the controls at 14 days of instillation (Fig. 5). Correspondingly, a significant increase ($\sim$38%) of GSSG level in the hippocampus of the 21 nm-Fe_2O_3 exposed mice was observed (Fig. 6). The significant elevations of GSSG level in the cortex and cerebellum were found in the 12 h and 72 h exposure group, respectively (Fig. 6). The GSH and GSSG in the olfactory bulb and hippocampus of the 280 nm-Fe_2O_3 instilled mice presented similar changes (Figs. 5, 6). However, in the cortex, cerebellum and brain stem of the mice, no significant changes of GSH and GSSG had been found (Figs. 5, 6).

Analysis of GSH/GSSG ratio revealed that the GSH/GSSG in the olfactory bulb of the 21 nm-Fe_2O_3 exposed mice significantly declined by 28% at 12 h and persisted till to the 72 h of instillation ($p < 0.05$). In contrast, though intranasally instilled 280 nm-Fe_2O_3 particles resulted in a significant decrease of GSH/GSSG ratio in the olfactory bulb as well ($p < 0.01$), the decrease was at the day 14 of instillation, which was much more delayed than in the 21 nm-Fe_2O_3 treated mice (Fig. 7). Moreover, the ratios of GSH/GSSG displayed a dose–effect response in the hippocampus of both 21 nm- and

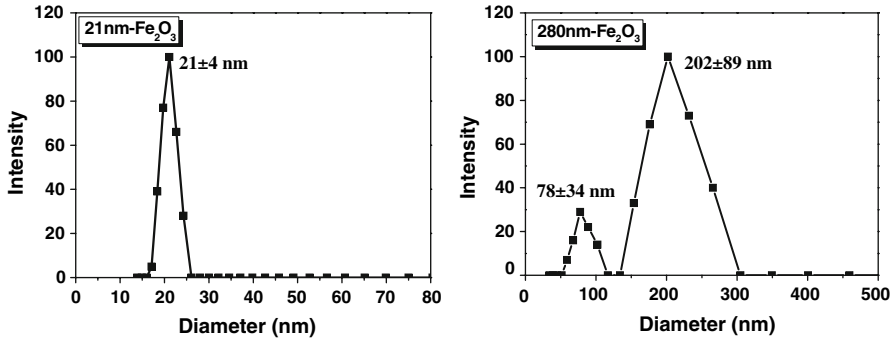

Fig. 3 Dynamic laser light scattering (DLS) analysis of hydrodynamic mean diameter of the 21 nm- and 280 nm-Fe_2O_3 particles in 0.1% sodium carboxy methyl cellulose

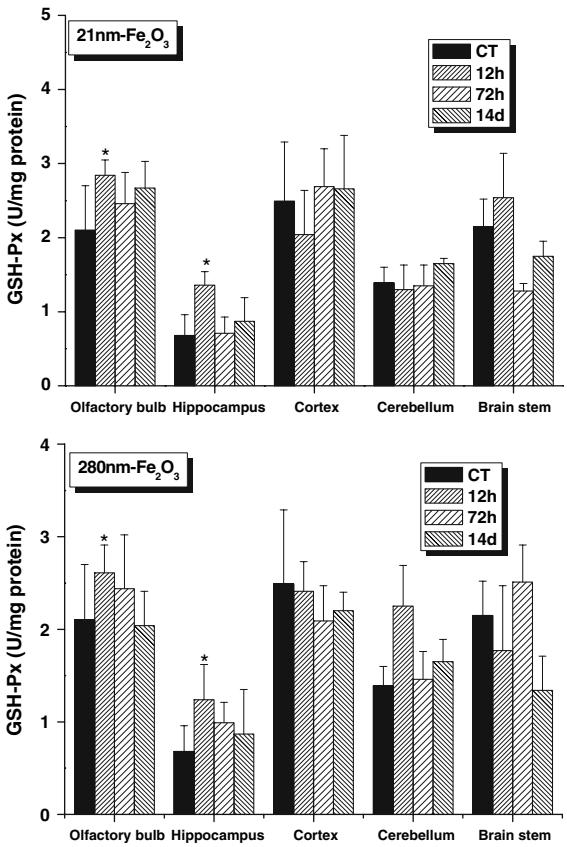

Fig. 4 GSH-Px activities in the brain regions of the mice exposed to the 21 nm- and 280 nm-Fe_2O_3 particles. $n = 6$. Dose: 130 μg Fe_2O_3 every other day. CT: control; 12 h: 12 h after instillation; 72 h: 72 h of instillation; 14 d: 14 days of instillation. The asterisk indicates the significant difference between the 21 nm- or 280 nm-Fe_2O_3 groups and the controls. (* $p < 0.05$; ** $p < 0.01$)

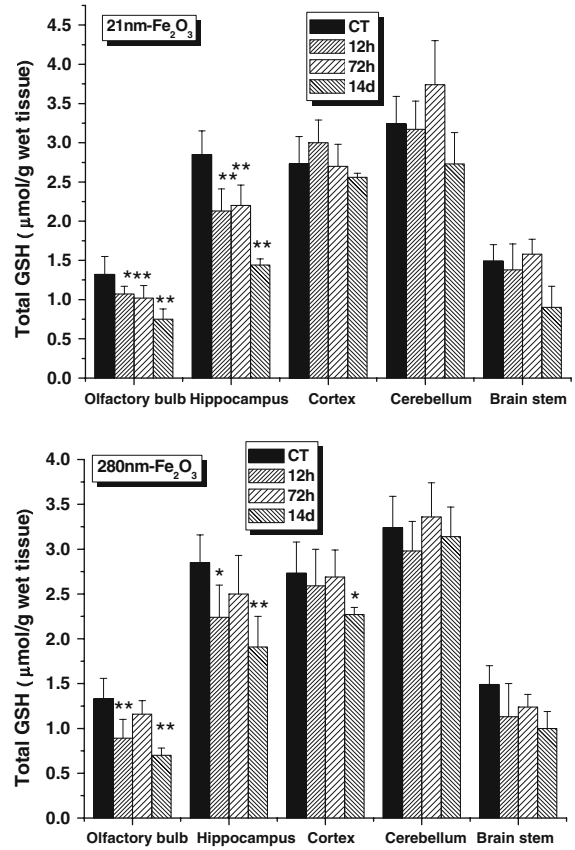

Fig. 5 Total GSH level in the brain regions of the mice exposed to the 21 nm- and 280 nm-Fe_2O_3 particles. $n = 6$. Dose: 130 μg Fe_2O_3 every other day. CT: control; 12 h: 12 h after instillation; 72 h: 72 h of instillation; 14 d: 14 days of instillation. The asterisk indicates the significant difference between the 21 nm- or 280 nm-Fe_2O_3 groups and the controls. (* $p < 0.05$; ** $p < 0.01$)

280 nm-Fe_2O_3 instilled mice. On day 14, the ratio of GSH/GSSG decreased by 66% and 46% in the 21 nm-and 280 nm-Fe_2O_3 instilled mice, respectively (Fig. 7).

The activities of Cu,Zn-SOD in the hippocampus were found to increase evidently after 30 days of instillation in both the 21 nm-and 280 nm-Fe_2O_3 treated mice ($p < 0.05$), corresponding to 145% and

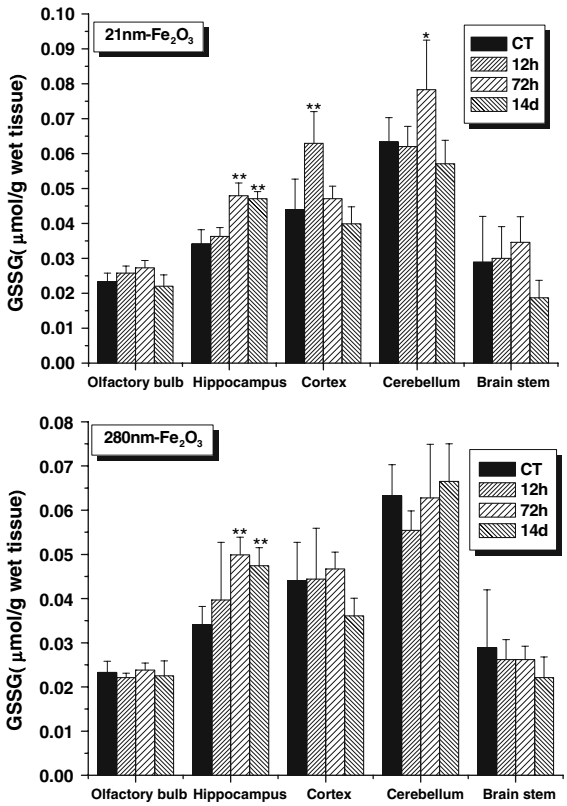

Fig. 6 GSSG level in the brain regions of the mice exposed to the 21 nm- and 280 nm-Fe_2O_3 particles. $n = 6$. Dose: 130 μg Fe_2O_3 every other day. CT: control; 12 h: 12 h after instillation; 72 h: 72 h of instillation; 14 d: 14 days of instillation. The asterisk indicates the significant difference between the 21 nm- or 280 nm-Fe_2O_3 groups and the controls. (* $p < 0.05$; ** $p < 0.01$)

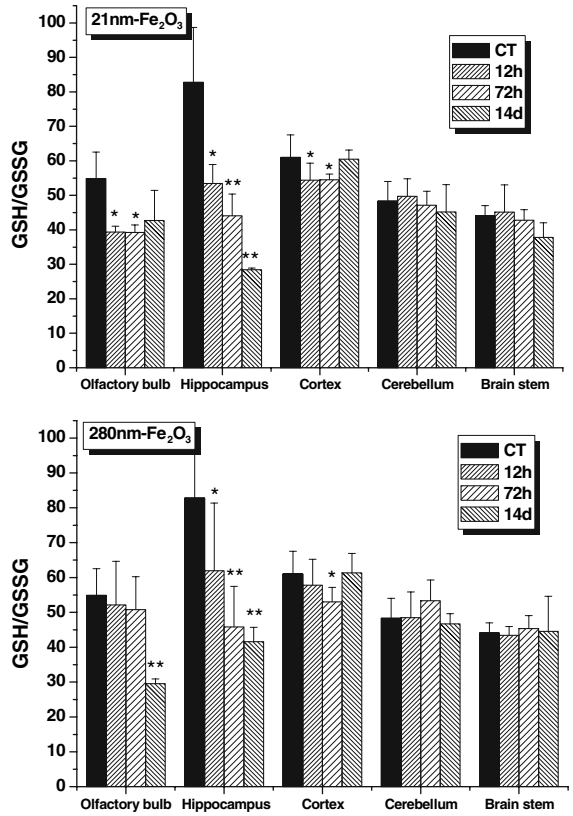

Fig. 7 Ratio of GSH to GSSG in the various brain regions of the mice exposed to the 21 nm- and 280 nm-Fe_2O_3 particles. $n = 6$. Dose: 130 μg Fe_2O_3 every other day. CT: control; 12 h: 12 h after instillation; 72 h: 72 h of instillation; 14 d: 14 days of instillation. The asterisk indicates the significant difference between the 21 nm- or 280 nm-Fe_2O_3 groups and the controls. (* $p < 0.05$; ** $p < 0.01$)

154% of control, respectively, while no significant changes were observed in other brain regions (Fig. 8a). No significant changes of Mn-SOD activities were found in all the observed brain regions when compared with the controls after instillation (Fig. 8b).

Assay of NOS activities revealed that instillation of the 21 nm- and 280 nm-Fe_2O_3 particles for 30 days resulted in a significant elevation of total NOS activities in the olfactory bulb, hippocampus and cerebellum (Table 1), which may mainly derived from the significant increase of cNOS activity (Table 1). The cNOS activities in the above brain samples of the 21 nm-Fe_2O_3 treated mice are generally higher than those in the 280 nm-Fe_2O_3 treated mice. No significant changes were found in the iNOS activities between the control and the exposed groups (Table 1).

The contents of TBARS in the brain regions of the 21 nm- or 280 nm-Fe_2O_3 instilled mice showed slight decrease in the hippocampus, cortex, cerebellum, and brain stem, but no significant differences were observed when compared with the controls (Fig. 9).

Monoamine neurotransmitter and their metabolites

The contents of monoamine neurotransmitter and related metabolites in the hippocampus of mice exposed to the 21 nm- and 280 nm-Fe_2O_3 particles were shown in Fig. 10. Compared with the controls, the levels of HIAA in the hippocampus of mice exposed to the 21 nm-Fe_2O_3 particles and NE in the hippocampus of mice exposed to the 280 nm-Fe_2O_3 particles decreased significantly ($p < 0.05$).

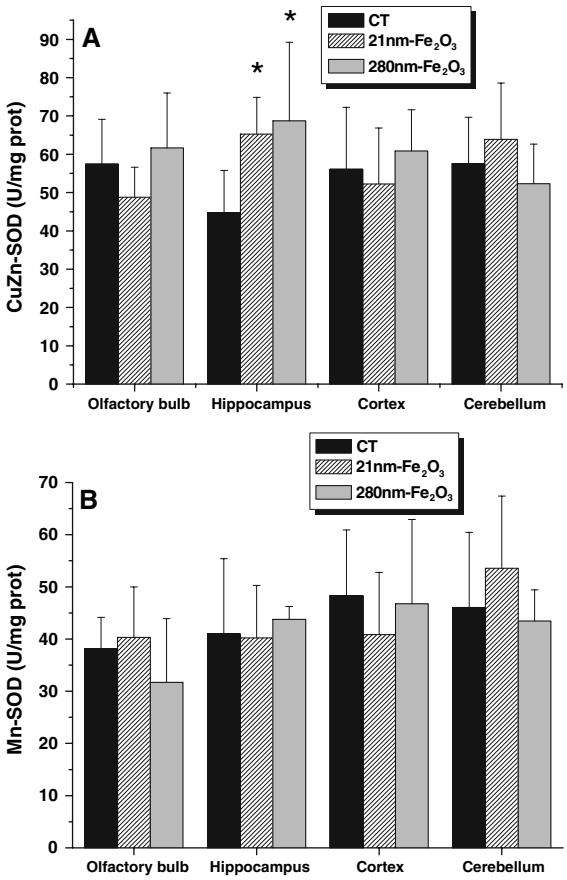

Fig. 8 SOD activities in the brain regions of the mice exposure to the 21 nm- and 280 nm-Fe_2O_3 particles for 30 days. $n = 6$. Dose: 130 μg Fe_2O_3 every other day. (**a**) Cu,Zn-SOD activities; (**b**) Mn-SOD activities. CT: control. (* $p < 0.05$)

Ultrastructural changes of nerve cells in brain

In the olfactory bulb section of the 21 nm-Fe_2O_3 exposed mice, nanoparticles were observed in the axon (Fig. 11a). The cell morphological changes of olfactory bulb, including slightly dilated rough endoplasmic reticulum, degeneration of neurodendron, disruption of membranous structure, and increase of lysosome of nerve cells, were induced by intranasal exposure to the 21 nm-Fe_2O_3 particles (Fig. 11a–c). Comparatively, in the 280 nm-Fe_2O_3 group mice, slightly swollen mitochondria of nerve cells were observed in the olfactory bulb (Fig. 11d).

The TEM image of hippocampus in the 21 nm-Fe_2O_3 instilled mice revealed that some nanoparticles

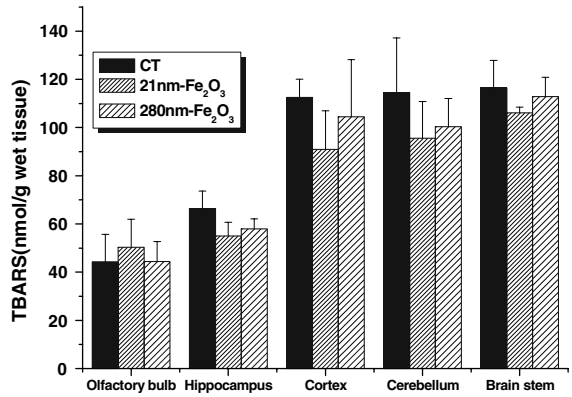

Fig. 9 TBARS content in the brain regions of the mice exposure to the 21 nm- and 280 nm-Fe_2O_3 particles for 30 days. $n = 6$. Dose: 130 μg Fe_2O_3 every other day. CT: control

Table 1 NOS activities in brain regions of mice intranasal exposure to 21 nm- and 280 nm-Fe_2O_3 particles for 30 days: $n = 6$ (U/mg protein)

NOS	Groups	Olfactory bulb	Hippocampus	Cerebrum	Cerebellum
TNOS	CT	0.46 ± 0.17	0.79 ± 0.38	0.42 ± 0.11	0.40 ± 0.17
	21 nm Fe_2O_3	1.36 ± 0.17**	1.20 ± 0.31*	0.45 ± 0.18	0.68 ± 0.18**
	280 nm Fe_2O_3	1.29 ± 0.06**	1.27 ± 0.37*	0.55 ± 0.09	0.63 ± 0.14**
cNOS	CT	0.28 ± 0.17	0.42 ± 0.17	0.22 ± 0.06	0.20 ± 0.03
	21 nm Fe_2O_3	1.08 ± 0.14**	0.82 ± 0.23**	0.21 ± 0.04	0.49 ± 0.17**
	280 nm Fe_2O_3	0.94 ± 0.29*	0.78 ± 0.29	0.30 ± 0.11	0.37 ± 0.13
iNOS	CT	0.28 ± 0.02	0.37 ± 0.08	0.20 ± 0.12	0.20 ± 0.05
	21 nm Fe_2O_3	0.31 ± 0.08	0.39 ± 0.14	0.24 ± 0.07	0.19 ± 0.05
	280 nm Fe_2O_3	0.35 ± 0.03	0.49 ± 0.17	0.25 ± 0.01	0.26 ± 0.04

CT: control

* $p < 0.05$; ** $p < 0.01$

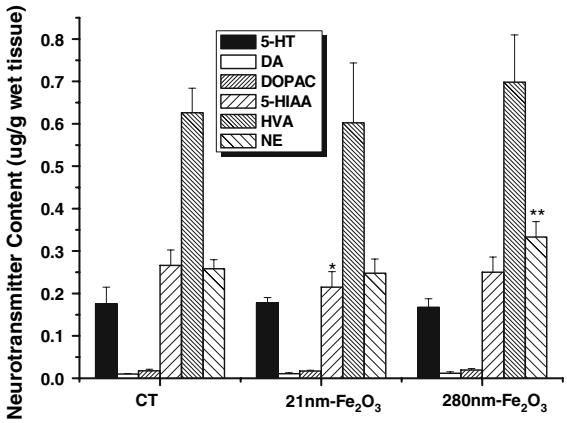

Fig. 10 Contents of monoamine neurotransmitters and their metabolites in the hippocampus of mice exposure to the 21 nm- and 280 nm-Fe_2O_3 particles for 30 days. $n = 6$. Dose: 130 μg Fe_2O_3 every other day. CT: control (* $p < 0.05$)

were located inside mitochondria, lysosome, and nearby the outer surface of the mitochondria membrane (Fig. 12a). Ultrastructural alteration of nerve cells, including slightly dilated rough endoplasmic reticulum and increased lysosome in the hippocampus (Fig. 12b) were observed in the 21 nm-Fe_2O_3 treated mice. In contrast, some vacuoles appeared in cell cytoplasm of the hippocampus in the 280 nm-Fe_2O_3 instilled mice (Fig. 12c).

Discussion

Based on our previous study that intranasally instilled iron oxide nanoparticles could transport into brain via olfactory route (Wang et al. 2007), we are highly concerned about the potential neurotoxicity of iron oxide nanoparticles in brain. The current knowledge about the toxicology for a variety of particles including environmental nanoparticles shows a close link between oxidative stress and diseases, such as cancer, asthma, and cardiovascular ailments (Long et al. 2006; Xia et al. 2006). The particle-induced oxidative stress

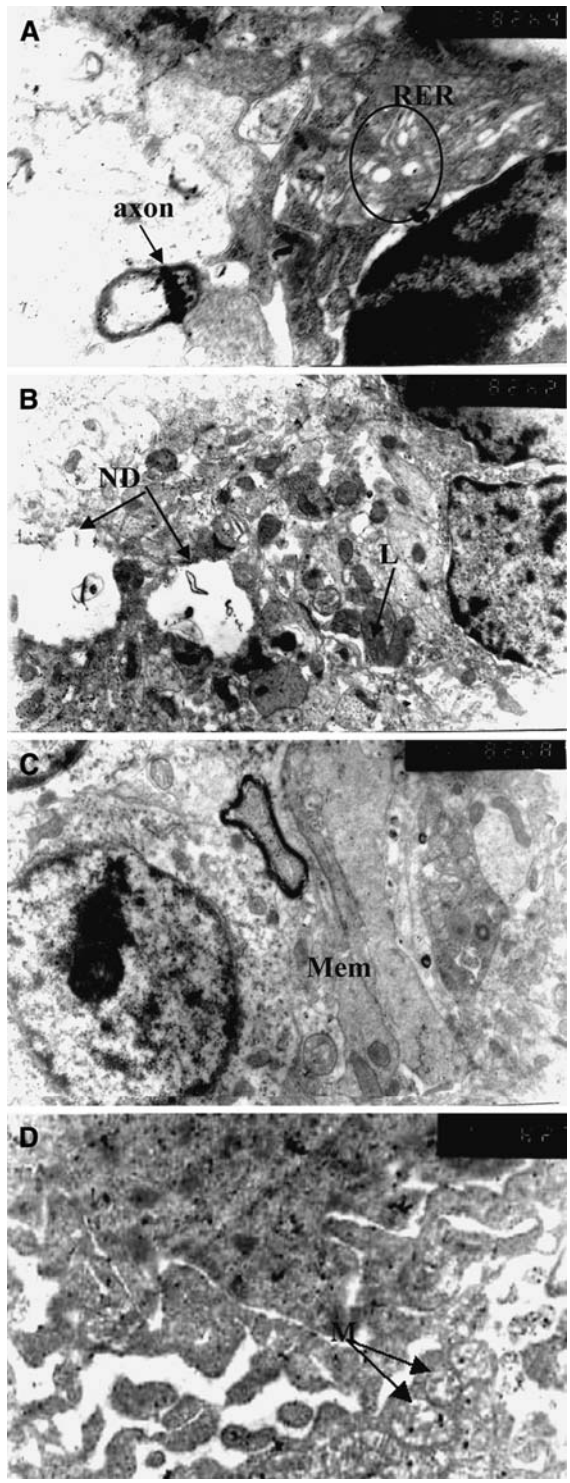

Fig. 11 TEM images of the olfactory bulb section in the mice exposure to the 21 nm (**a**–**c**) or 280 nm-Fe_2O_3 (**d**) for 30 days. (**a**) Nanoparticles were observed in the axon of the olfactory bulb for the 21 nm-Fe_2O_3 instilled mice. Circle indicates slight dilation of rough endoplasmic reticulum, magnification: ×20000; (**b**) degeneration of neurodendron and the increase of lysosome were found in the olfactory bulb of the 21 nm-Fe_2O_3 instilled mice. ND: neurodendron; L: lysosome, magnification: ×8000; (**c**) disruption of membranous structure in the olfactory bulb was induced by the 21 nm-Fe_2O_3 particles, magnification: ×10000. Mem: membrane; (**d**) slightly swollen mitochondria were observed in the 280 nm-Fe_2O_3 instilled mice, magnification: ×14000. M: mitochondria ▶

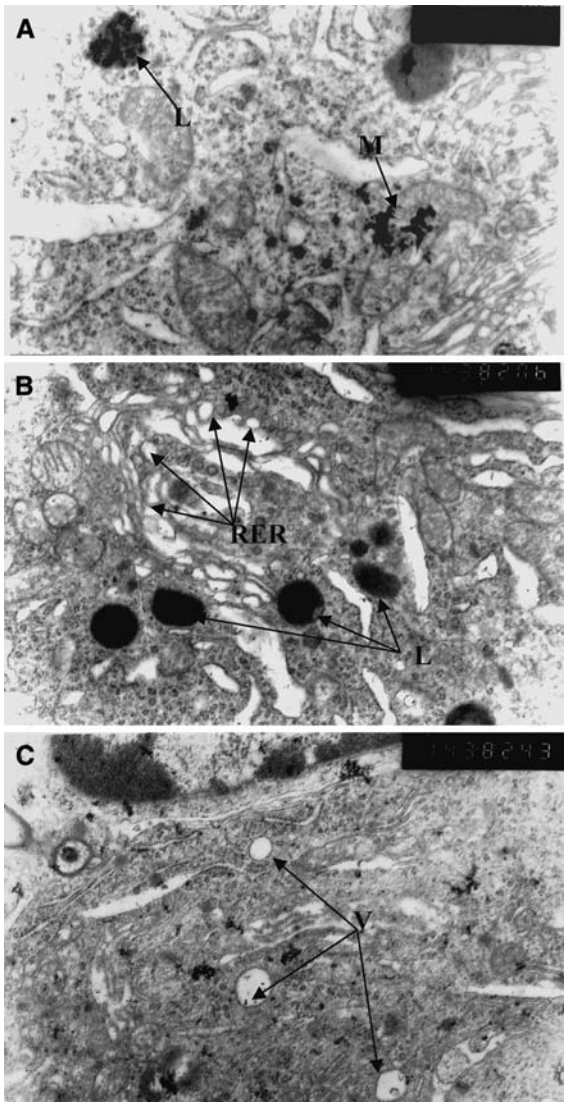

Fig. 12 TEM images of the hippocampus section in the mice exposure to the 21 nm- or 280 nm-Fe_2O_3 for 30 days. (**a**) Some particles were present inside mitochondria and lysosome, and nearby the outer surface of the mitochondria membrane. L: lysosome; M: mitochondria, magnification: ×20000; (**b**) slight dilation of rough endoplasmic reticulum and the increase of lysosome were observed in the hippocampus for 30 days exposure to the 21 nm-Fe_2O_3 particles, magnification: ×14000, L: lysosome; RER: rough endoplasmic reticulum; (**c**) several vacuoles appeared in the nerve cell cytoplasm of the mice for 30 days exposure to the 280 nm-Fe_2O_3 particles, V: vacuoles

has been considered as one of the important mechanism of nanotoxicology (Shvedova et al. 2005; Nel et al. 2006). Several clinical and experimental studies have demonstrated that nanoparticles with a small size and large surface area had an ability to generate reactive oxygen species (ROS) (Donaldson and Stone 2003; Li et al. 2003; Xia et al. 2006; Wörle-Knirsch et al. 2007). Li et al. (2003) demonstrated that ultrafine particles are the most potent toward inducing depleting glutathione in macrophages. Iron as a redox-active transition metal is hypothesized to contribute the formation of reactive oxygen species (ROS) and modulate oxidative stress level. It has been demonstrated that acute exposure to ultrafine iron particles resulted in a significant decrease in total antioxidant power in the lung (Zhou et al. 2003).

Brain tissue is rich in polyunsaturated lipids and has high iron content, thus, highly vulnerable to ROS mediated oxidative damage (Siegel et al. 1985). In many neurodegenerative disorders, including Hallervorden–Spatz Syndrome, Parkinson's and Alzheimer's diseases, iron excessively accumulated in the brain has been shown to respond for the oxidative stress and neuronal death (Aisen et al. 1999; Sayre et al. 1999; Qian and Shen 2001). Previous reports indicate that the iron concentration in amigdala, pyriform cortex, hippocampus and olfactory region elevated obviously in Alzheimer's disease (Samudralwer et al. 1995; Deibel et al. 1996). Recently, Hautot et al. (2007) demonstrated that the elevated levels of nanocrystalline iron oxide were observed in the basal ganglia of neuroferritinopathy patients. Our previous study demonstrated that the 21 nm- and 280 nm-Fe_2O_3 particles were almost insoluble as long as 24 h in the 0.1% SCMC saline solution (pH 7.3) and artificial cerebrospinal fluid (ACSF, pH 7.7) (data will be published elsewhere). Additionally, the TEM image directly showed the Fe_2O_3 particle accumulated in the olfactory bulb and hippocampus (Figs. 9a, 10a). Therefore, we considered whether the slow soluble or insoluble iron nanoparticle could cause similar neurotoxicity as the iron ion in brain.

In this work, from the results of the oxidative-stress-related biochemical measurement and the ultrastructural changes of nerve cells in the hippocampus and olfactory bulb, we suggest that the oxidative stress may occur in the CNS after the nano- and submicron-sized Fe_2O_3 particles translocation. The significant elevation of GSH-Px activities in the olfactory bulb and hippocampus at 12 h post-instillation and significant increase of SOD activities at 30 days in hippocampus reflect the oxidative stress

response to the exposure of both 21 nm- and 280 nm-Fe_2O_3 particles. The significant decrease of total GSH level and GSH/GSSG ratio in the olfactory bulb and hippocampus indicates a decreased reductive capacity and antioxidation after exposure. The depletion of GSH is usually used as an indicator of oxyradical scavenging ability, indicating that the antioxidant defense system is overwhelmed by ROSs. The previous work showed that GSH was marginally depleted in gill of the fullerenes (C_{60}) exposed fish (Oberdörster 2004). As in this work, the significant decrease of total GSH level and GSH/GSSG ratio in the olfactory bulb and hippocampus suggests that the system is beginning to lose its ability to maintain the critical balance of the redox states after the 21 nm- and 280 nm-Fe_2O_3 exposure. The greater decrease and significant dose–effect response of GSH/GSSG ratio in the hippocampus of the 21 nm-Fe_2O_3 group mice than in the 280 nm-Fe_2O_3 treated mice suggests that the 21 nm-Fe_2O_3 particle is easier to arouse oxidative stress than the 280 nm-Fe_2O_3 particle does, which corresponds with the extent of nerve cell injury observed in the 21 nm-Fe_2O_3 and 280 nm-Fe_2O_3 instilled mice. This size-dependent manner was also demonstrated by the study of intranasal instillation of carbon black (CB) nanoparticles in mice that the expression of cytokine and chemokine mRNA of the olfactory bulb was induced only in the 14 nm-CB treated mice but not in the 95 nm-CB treated ones (Tin-Tin-Win-Shwe et al. 2006). No significant changes of TBARS (the product of lipid peroxidation) at 30 days of Fe_2O_3 particle instillation in the CNS indicated that glutathione might effectively combat with lipid peroxides in the cells and thus, exerted a protective effect against oxidative stress.

The significant elevation of cytosolic Cu,Zn-SOD activity in the hippocampus at 30 days of instillation indicates the production of superoxide anion (O_2) has increased, thus, active SOD to detoxify superoxide anion into other potent oxidants, such as hydrogen peroxide, hydroxyl radical, and peroxynitrite. The higher levels of SOD may shift signaling to peroxide-linked mechanisms of inflammation and diseases.

It has been demonstrated that $NO^{\bullet}$ plays double-edged roles in either neurotoxicity or neuroprotection under the oxidative stress (Hölscher 1997; Lin 1999; Prast and Philippu 2001). NO can quickly react with superoxide anion resulting in the formation of the peroxynitrite anion ($ONOO^-$), which is extremely cytotoxic (Lipton et al. 1993). It is reported that the depletion of brain GSH results in increased nitric oxide synthase (Heales et al. 1996). However, since $NO^{\bullet}$ is highly unstable and difficult to study directly, therefore, in this study we investigated the effects of Fe_2O_3 particles exposure on the activity of constitutive nitric oxide synthase (cNOS) and inducible nitric oxide synthase (iNOS), which are the rate-limiting enzymes for synthesis of NO to indirectly reflect the changes of NO in the different brain regions of mice. Exocytoic Ca^{2+} can stimulate cNOS to activate (Hölscher 1997), suggesting that cNOS may respond quickly to tissue injury. Therefore, in our study, accompanying with the decrease of GSH level in the olfactory bulb and hippocampus, the elevated cNOS activities might indicate the protective effect for the exposure of Fe_2O_3 particles. Versus the 280 nm-Fe_2O_3 particle exposure, the 21 nm particle induced greater increase of cNOS activity.

Some studies have indicated that stress reaction could change the monoamine neurotransmitter level of brain in the mice (Papaioannou et al. 2002). It has been demonstrated that manganese oxide nanoparticles (40 nm) would induce dopamine (DA) depletion in a cultured neuronal PC-12 cells and this process might be related with increased reactive oxygen species (ROS) (Hussain et al. 2006). The slight change of HIAA and NE level in the hippocampus of mice exposed to the 21 nm- and 280 nm-Fe_2O_3 particles might indicate a potential impact on monoamine neurotransmitter level of brain.

There were also subcellular reactions in the brain of nano- and submicron-sized Fe_2O_3 particle treated mice. Carefully ultrastructural observation indicated that more severe morphological signs of cell damage were induced by the 21 nm-Fe_2O_3 treatment than by the 280 nm one. The slightly swollen mitochondrion and slightly dilated rough endoplasmic reticulum of nerve cells in the olfactory bulb and hippocampus might be a compensation reaction for oxidative stress. It has been demonstrated that nanoparticles of various sizes and various chemical compositions preferentially mobilize to mitochondria (DeLorenzo 1970; Foley et al. 2002; Li et al. 2003; Rodoslav et al. 2003). Recently, Long et al. (2006) reported that titanium oxide nanoparticles induced swollen and disrupted mitochondria membrane of microglia as well. Lysosomes with strong digestive enzymes can digest waste materials, food and damaged organelle

within the cell, and break down molecules into their base components. The presence of elevated amount of lysosomes may reflect an enhanced phagocytosis function for exogenous particle exposure.

In the present work, we investigate the neurotoxicity of intranasal exposure of unmodified nano- and submicron-sized Fe_2O_3 particles, however, depending on the unique properties of nanoparticles, the physicochemical properties of the particles such as shape, surface properties (area, porosity, charge, and surface modifications), and the crystal structure on the effect of CNS are unknown yet. Considering the great progress of iron nanoparticle application study, comprehending the behavior of the materials in living system will have implications not only for safety consideration but also for their valid application, e.g., drug delivery design and disease treatment in the future.

Conclusions

We conclude from our results that low-dose repeatedly intranasal instillation of nano- and submicron-sized Fe_2O_3 particles resulted in oxidative stress response and morphological signs of cell damage in the sensitive brain regions. The alternations of GSH/GSSG, cNOS, and cell morphology indicate that 21 nm-Fe_2O_3 particles may induce more severe oxidative stress and cell injury in brain than 280 nm-Fe_2O_3 does. These are the first results to clarify the neurotoxicity of nano- and submicron-sized Fe_2O_3 intranasal exposure in vivo, which are of important significance for environmental or occupational safety following inhalation exposure to iron nanoparticles. Therefore, our work arouses the attention of iron oxide nanoparticle application and exposure effects especially on human brain for long-term and low-dose treatment.

Acknowledgments The authors are grateful to the foundations of MOST 973 program (2006CB705605, 2007CB935604, and 2006CB932505), the Chinese Academy of Sciences (KJCX3.SYW.N3) and the National Natural Science Foundation of China (10490181, 10675139, and 10525524).

References

Aisen P, Wessling-Resnick M, Leibold EA (1999) Iron metabolism. Curr Opin Chem Biol 3:200–206. doi:10.1016/S1367-5931(99)80033-7

Au WW, Treloar HB, Greer CA (2002) Sublaminar organization of the mouse olfactory bulb nerve layer. J Comp Neurol 446:68–80. doi:10.1002/cne.10182

Baker MA, Cerniglia GJ, Zaman A (1990) Microtiter plate assay for the measurement of glutathione and glutathione disulfide in large numbers of biological samples. Anal Biochem 190:360–365. doi:10.1016/0003-2697(90)90208-Q

Bradford MM (1976) A rapid and sensitive method for the quantitation of microgram quantities of protein utilizing the principle of protein-dye binding. Anal Biochem 72:248–254. doi:10.1016/0003-2697(76)90527-3

Bush AI (2003) The metallobiology of Alzheimer's disease. Trends Neurosci 26:207–214. doi:10.1016/S0166-2236(03)00067-5

Deibel MA, Ehmann WD, Markesbery WR (1996) Copper, iron and zinc imbalances in severely degenerated brain regions in Alzheimer's disease: possible relation to oxidative stress. J Neurol Sci 143:137–142. doi:10.1016/S0022-510X(96)00203-1

DeLorenzo A (1970) The olfactory neuron and the blood-brain barrier. In: Wolstenholme G, Knight J (eds) Taste and smell in vertebrates CIBA foundation symposium series. J&A Churchill, London, pp 151–176

Donaldson K, Stone V (2003) Current hypotheses on the mechanisms of toxicity of ultrafine particles. Ann Ist Super Sanita 39(3):405–410

Donaldson K, Stone V, Clouter A, Renwick L, MacNee W (2001) Ultrafine particles. Occup Environ Med 58:211–216. doi:10.1136/oem.58.3.211

Elder A, Gelein R, Silva V, Feikert T, Opanashuk L, Carter J et al (2006) Translocation of inhaled ultrafine manganese oxide particles to the central nervous system. Environ Health Perspect 114(8):1172–1178

Flohe L, Gunzler WA (1984) Glutathione peroxidase. Methods Enzymol 105:115–121

Foley S, Crowley C, Smaihi M, Bonfils C, Erlanger BF, Seta P et al (2002) Cellular localization of a water-soluble fullerene derivative. Biochem Biophys Res Commun 294:116–119. doi:10.1016/S0006-291X(02)00445-X

Hautot D, Pankhurst QA, Morris CM, Curtis A, Burn J, Dobson J (1772/2007) Preliminary observation of elevated levels of nanocrystalline iron oxide in the basal ganglia of neuroferritinopathy patients. Biochim Biophys Acta (1):21–25

Heales SJR, Bolafios JP, Clark JB (1996) Glutathione depletion is accompanied by increased neuronal nitric oxide synthase activity. Neurochem Res 21(1):35–39. doi:10.1007/BF02527669

Hoet PHM, Brüske-Hohlfeld I, Salata OV (2004) Nanoparticles—known and unknown health risks. J Nanobiotechnol 2:12–27. doi:10.1186/1477-3155-2-12

Hölscher C (1997) Nitric oxide, the enigmatic neuronal messenger: its role in synaptic plasticity. Trends Neurosci 20:298–303. doi:10.1016/S0166-2236(97)01065-5

Horányi G, Kálmán E (2004) Anion specific adsorption on Fe_2O_3 and AlOOH nanoparticles in aqueous solutions: comparison with hematite and γ-Al_2O_3. J Colloid Interface Sci 269:315–319. doi:10.1016/S0021-9797(03)00750-1

Hussain SM, Javorina AK, Schrand AM, Duhart HM, Ali SF, Schlager JJ (2006) The interaction of manganese nanoparticles with PC-12 cells induces dopamine depletion. Toxicol Sci 92(2):456–463. doi:10.1093/toxsci/kfl020

Li N, Sioutas C, Cho A, Schmitz D, Misra C, Sempf J et al (2003) Ultrafine particulate pollutants induce oxidative stress and mitochondrial damage. Environ Health Perspect 111:455–460

Lin AMY (1999) Recovery by NO of the iron-attenuated dopamine dynamics in nigrostriatal system of rat brain. Neurosci Res 34:133–139. doi:10.1016/S0168-0102(99)00054-1

Lipton SA, Choy YB, Pan ZH, Lei SZ, Chen HS, Sucher NJ et al (1993) A redox-based mechanism for the neuroprotective effects of nitric oxide and related nitroso-compounds. Nature 364:626–632. doi:10.1038/364626a0

Long TC, Saleh N, Tilton RD, Lowry GV, Veronesi B (2006) Titanium dioxide (P25) produces reactive oxygen species in immortalized brain microglia (BV2): implications for nanoparticle neurotoxicity. Environ Sci Technol 40(14):4346–4352. doi:10.1021/es060589n

MacNee W, Donaldson K (2003) Mechanism of lung injury caused by PM10 and ultrafine particles with special reference to COPD. Eur Respir J Suppl 40:47s–51s. doi:10.1183/09031936.03.00403203

Maynard AD, Kuempel ED (2005) Airborne nanostructured particles and occupational health. J Nanopart Res 7:587–614. doi:10.1007/s11051-005-6770-9

Misra HP, Fridovich I (1972) The role of superoxide anion in the autooxidation of the epinephrine and a sample assay for superoxide dismutase. J Biol Chem 247:3170–3175

Nel A, Xia T, Mädler L, Li N (2006) Toxic potential of materials at the nanolevel. Science 311:622–627

Nemmar A, Vanbilloen H, Hoylaerts MF, Hoet PHM, Verbruggen A, Nemery B (2001) Passage of intratracheally instilled ultrafine particles from the lung into the systemic circulation in hamster. Am J Respir Crit Care Med 164:1665–1668

Oberdörster E (2004) Manufactured nanomaterials (Fullerenes, C60) induce oxidative stress in the brain of juvenile largemouth bass. Environ Health Perspect 112(10):1058–1062

Oberdörster G, Sharp Z, Atudorei V, Elder A, Gelein R, Kreyling W (2004) Translocation of inhaled ultrafine particles to the brain. Inhal Toxicol 16(6–7):437–445. doi:10.1080/08958370490439597

Ohkawa H, Ohishi N, Yagi K (1979) Assay for lipid peroxides in animal tissues by thiobarbituric acid reaction. Anal Biochem 95:351–358. doi:10.1016/0003-2697(79)90738-3

Papaioannou A, Dafni U, Alikaridis F, Bolaris S, Stylianopoulou F (2002) Effects of neonatal handling on basal and stress-induced monoamine levels in the male and female rat brain. Neuroscience 114(1):195–206. doi:10.1016/S0306-4522(02)00129-X

Penpolcharoen M, Amal R, Brungs M (2001) Degradation of sucrose and nitrate over titania coated nano-hematite photocatalysts. J Nanopart Res 3:289–302. doi:10.1023/A:1017929204380

Peters A, Wichmann HE, Tuch T, Heinrich J, Heyder J (1997) Respiratory effects are associated with the number of ultrafine particles. Am J Respir Crit Care Med 155:1376–1383

Pisanic TRII, Blackwell JD, Shubayev VI, Fiñones RR, Jin S (2007) Nanotoxicity of iron oxide nanoparticle internalization in growing neurons. Biomaterials 28:2572–2581. doi:10.1016/j.biomaterials.2007.01.043

Prast H, Philippu A (2001) Nitric oxide as modulator of neuronal function. Prog Neurobiol 64:51–68. doi:10.1016/S0301-0082(00)00044-7

Qian ZM, Shen X (2001) Brain iron transport and neurodegeneration. Trends Mol Med 7:103–108. doi:10.1016/S1471-4914(00)01910-9

Rodoslav S, Laibin L, Eisenberg A, Dusica M (2003) Micellar nanocontainers distribute to defined cytoplasmic organelles. Science 300:615–618. doi:10.1126/science.1078192

Salter M, Knowles RG, Moncada S (1991) Widespread tissue distribution, species distribution and changes in activity of Ca^{2+}-dependent and Ca^{2+}-independent nitric oxide synthases. FEBS Lett 291:145–149. doi:10.1016/0014-5793(91)81123-P

Samudralwer DL, Diprete CC, Ni BF, Ehmann WD, Markesbery WR (1995) Elemental imbalances in the olfactory pathway in Alzheimer's disease. J Neurol Sci 130:139–145. doi:10.1016/0022-510X(95)00018-W

Sayre LM, Perry G, Smith MA (1999) Redox metals and neurodegenerative disease. Curr Opin Chem Biol 3:220–225. doi:10.1016/S1367-5931(99)80035-0

Schulz JB, Matthews RT, Jenkins BG, Ferrante RJ, Siwek D, Henshaw DR et al (1995) Blockade of neuronal nitric oxide synthase protects against excitotoxicity in vivo. J Neurosci 15:8419–8429

Shvedova AA, Kisin ER, Mercer R, Murray AR, Johnson VJ, Potapovich AI et al (2005) Unusual inflammatory and fibrogenic pulmonary responses to single walled carbon nanotubes in mice. Am J Physiol Lung Cell Mol Physiol 289:L698–L708. doi:10.1152/ajplung.00084.2005

Siegel GJ, Agranoff BW, Albers RW, Fischer SK, Uhler MD (eds) (1985) Basic neurochemistry: molecular, cellular and medical aspects, 6th edn. Lippincott Raven, Philadelphia

Sun Y, Oberley LW, Li Y (1988) A simple method for clinical assay of superoxide dismutase. Clin Chem 34(3):497–500

Thompson KJ, Shoham S, Connor JR (2001) Iron and neurodegenerative disorders. Brain Res Bull 55:155–164. doi:10.1016/S0361-9230(01)00510-X

Tin-Tin-Win-Shwe, Yamamoto S, Ahmed S, Kakeyama M, Kobayashi T, Fujimaki H (2006) Brain cytokine and chemokine mRNA expression in mice induced by intranasal instillation with ultrafine carbon black. Toxicol Lett 163(2):153–160. doi:10.1016/j.toxlet.2005.10.006

Utell MJ, Frampton MW (2000) Acute health effects of ambient air pollution: the ultrafine particle hypothesis. J Aerosol Med 13:355–359

Wang B, Feng WY, Wang M, Shi JW, Zhang F, Ouyang H et al (2007) Transport of intranasally instilled fine Fe_2O_3 particles into the brain: micro-distribution, chemical states, and histopathological observation. Biol Trace Elem Res 118:233–243. doi:10.1007/s12011-007-0028-6

Wörle-Knirsch JM, Kern K, Schleh C, Adelhelm C, Feldmann C, Krug HF (2007) Nanoparticulate vanadium oxide potentiated vanadium toxicity in human lung cells. Environ Sci Technol 41(1):331–336. doi:10.1021/es061140x

Xia T, Kovochich M, Brant J, Hotze M, Sempf J, Oberley T et al (2006) Comparison of the abilities of ambient and manufactured nanoparticles to induce cellular toxicity according to an oxidative stress paradigm. Nano Lett 6(8):1794–1807. doi:10.1021/nl061025k

Zhou YM, Zhong CY, Kennedy IM, Pinkerton KE (2003) Pulmonary responses of acute exposure to ultrafine iron particles in healthy adult rats. Environ Toxicol 18:227–235. doi:10.1002/tox.10119